Orientational Order of the Water Molecules Across a Fully Hydrated DMPC Bilayer: A Monte Carlo Simulation Study

Pál Jedlovszky[†] and Mihaly Mezei*

Department of Physiology and Biophysics, Mount Sinai School of Medicine, New York University, New York, New York 10029

Received: March 28, 2000; In Final Form: January 24, 2001

The orientational order of water molecules located in different regions of a fully hydrated dimyristoylphosphatidylcholine (DMPC) membrane is analyzed and compared to that in pure water on the basis of an all-atom Monte Carlo simulation. The preferential orientation of the water molecules relative to the membrane as well as the relative orientation and hydrogen-bonding structure of neighboring molecules is discussed in detail. Due to the distribution of the charged groups of the lipid molecules, the water molecules in the interfacial region of the membrane are turning preferentially toward the membrane interior with their dipole moments, whereas in the hydrocarbon region the water dipoles are pointing toward the aqueous phase. The density of the water molecules in the hydrocarbon phase is found to be rather inhomogeneous; the few water molecules in this region are grouping together and form small hydrogen-bonded clusters. The long, mostly parallel lipid tails are forcing these water molecules to be aligned in planes parallel with them and also the hydrogen-bonded neighbors to be arranged around each other in a coplanar way. It is found that the relative importance of the interstitial molecules, which left the hydrogen-bonded network of the other molecules and are located in its cavities, increases considerably upon the approach of the molecules to the middle of the membrane. It is also found that the geometry of the hydrogen bond around the bonding H atom does not change noticeably across the bilayer, whereas when the molecules approach the membrane interior, the arrangement of the hydrogen-bonded neighbors around each other becomes less and less tetrahedral, until this preference for tetrahedral arrangement disappears completely.

Introduction

Water is a system of key importance in many areas of science.[1,2] Besides its importance in chemistry and physics as an excellent polar solvent of many substances and medium of various chemical reactions and as a liquid exhibiting anomalous thermodynamic properties, its vital biological importance comes from the fact that it is the medium of life. All of these unique properties of water are based on its peculiar molecular-level structure, which is determined by the dual ability of the water molecules of both forming a tetrahedral network connected by especially strong hydrogen bonds and also leaving this network and being located in its cavities.[3−6]

The local structure around individual water molecules has also a key effect on the structure and thus the function of molecular assemblies of vital biological importance. Examples for such assemblies are lipid membranes and membrane-bound protein molecules, which separate living cells from the outside environment and regulate their metabolism. Due to their rather complex structure, these membranes have an amphiphilic character. Their outer phase contains strongly polar or even zwitterionic groups, whereas in their middle region apolar hydrophobic hydrocarbon chains can be found. The presence of such amphiphilic structures themselves is already the consequence of the water properties. Moreover, the change of the orientational ordering and local structure of the water molecules determines the variation of the dielectric properties across the membrane, and thus has a great influence on the crossmembrane transport properties of charged and dipolar particles. Although ions usually cross the cell membrane with the aid of specific channel-forming proteins,[7] the free energy barrier of their direct transport across the membrane can also have biological relevance. Namely, the lower this barrier is the higher is the importance of their passive transport, as well. Moreover, several neutral but dipolar molecules of biological importance, such as water itself, methanol, formamide, or urea can permeate the cell membrane simply by diffusion.[8,9] The dielectric properties, and thus the local water structure, can also have an effect on the structure of the membrane-bound protein molecules by influencing the ionization state and conformation of their side chains as well as the spatial distribution of the side chains of various polarity.

While it is rather difficult to obtain direct information on the local ordering of the water molecules at different parts of the membrane by experimental methods, it can be investigated in detail by computer simulation. Various different kinds of lipid membranes (e.g., ones consisting of zwitterionic[10−25] or charged[26] headgroups, having unsaturated,[11,17] branching,[19] or fluorinated[21] side-chains, containing cholesterol,[13,16] transmembrane helix,[22] or a DNA segment,[23] etc.) have already been successfully simulated, and the resulting structures have also been analyzed in various respects. Thus, the conformation of the hydrocarbon chains[17,21] the water-separated[18] and contact[20] ion−ion interactions in the headgroup region, the orientation of the headgroup dipole moment,[17,19,20] the penetration of the water molecules into the hydrocarbon region,[12,14,18,24] as well as the crossmem-

* Author for correspondence. E-mail: mezei@inka.mssm.edu.
[†] E-mail: pali@inka.mssm.edu. Present address: Department of Chemical Information, Technical University of Budapest, Hungary.

10.1021/jp001175y CCC: $20.00
Published on Web 04/04/2001

brane free energy profile of several small molecules[12,25] have been investigated. Various calculated structural properties, such as the average area per headgroup,[14,19−22] the deuterium order parameters of the side chains[11,14,15,17,22,26] and electron density profiles[19,22] have also been compared with experimental data. Several studies have also been focused on the dipolar orientation of the water molecules relative to the water−lipid interface both in lipid mono-[27,28] and bilayers.[17,29,30] However, the effect of the membrane on the orientation of the water molecules relative to each other has, to our knowledge, not been studied yet in detail.

In this paper, we report results of a Monte Carlo simulation of a fully hydrated bilayer of dimyristoylphosphatidylcholine (DMPC) molecules and analyze the local ordering of the water molecules located in the different regions of this membrane in various respects. These analyses include the investigation of the orientation of the water molecules relative to the bilayer (i.e., a space-fixed reference frame) as well as relative to their neighbors (i.e., in a local frame), the geometry of the hydrogen bonds, and the spatial distribution of the neighboring molecules around each other. Partial pair correlation functions and the coefficients of the spherical harmonic expansion of the orientational pair correlation function are also analyzed. To clarify the role of the lipid molecules in determining the local water structure, all of the analyses have also been performed on pure water as a reference system.

The paper is organized as follows. In the next section details of the simulation performed are given. Then, the results obtained are presented and discussed in detail. Finally, some conclusions are drawn.

Monte Carlo Simulations. Monte Carlo simulation of a fully hydrated DMPC bilayer has been performed using the program MMC[31] in the (*N*, *p*, *T*) ensemble at 1 bar and 310 K, well above the gel/liquid crystalline transition temperature. The two DMPC layers have contained 25−25 lipid molecules each, and the bilayer has been hydrated by 2033 water molecules. To maximize the distance between two periodic images of the lipid molecules in the quasi-planar layers, a hexagonal prism-shaped basic simulation cell has been used, with the hexagonal faces being parallel to the plane of the two lipid layers.

The DMPC molecules have been described by the all-atom CHARMM22 force field optimized for phospholipids,[32] whereas the water molecules have been represented by the three-site TIP3P model.[33] To avoid simulating an infinite stack of lipid bilayers, the long-range part of the interactions have been treated by group-based spherical cutoffs. The sum of partial charges on each group was zero. Water−water and water−lipid interactions have been truncated to zero beyond the center-center distance of 12 Å and 20 Å, respectively. This combination was found to behave close to the "infinite" cutoff system for a hydrated lipid monolayer.[27] For the lipid−lipid interactions group-based minimum image convention was used.

The conformation of the DMPC molecules have been sampled from their torsion angle space, whereas their bond lengths and bond angles have been kept fixed at their equilibrium values in the simulation. Water and lipid moves have been performed in an alternating order, and every 1250 of them has been followed by a volume-changing step. In a water move a randomly chosen molecule has been translated by a random distance below 0.3 Å and rotated by no more than 20° around a randomly selected space-fixed axis. In a lipid move (with 80% probability) either one of the torsional angles of the selected molecule has been changed, or, with 20% probability, an entire DMPC molecule has been translated and rotated. Lipid molecules have been selected in a shuffled cyclic order[34] both for displacement and torsional angle change. The moved torsional angles have been selected sequentially, going from the end of a chain toward the center of the lipid molecule, but subject to a probability filter, allowing more frequent torsional moves far from the end of the chains. The torsional angle changes as well as the overall lipid rotations have been performed using the novel extension-biased method.[24] In this way, the maximum angle of rotation $\Delta\Psi_{max}$ has been determined for each individual rotation as

$$\Delta\Psi_{max} = \frac{c}{\sqrt{R_{max}}} \tag{1}$$

where c is the stepsize parameter, which is kept fixed in the entire simulation, and R_{max} is the distance of the farthest rotated atom from the rotation axis. The stepsize parameter c has been optimized for each of the 41 torsions as well as for the overall lipid rotations, as described in detail in our previous paper.[24] The details of the optimization as well as the final stepsize parameter values and the values of the probability filter for the torsional angle selection have been summarized elsewhere.[35]

In a volume change move either the edge length of the basic hexagon or the length of the edge perpendicular to it (i.e., either the cross-section or the height of the hexagonal prism-shaped simulation cell) has been changed, in an alternating order. In this way, the surface density of the lipid molecules and the volume density of the entire system have been allowed to equilibrate independently from each other, ensuring that the pressure in the direction normal to the bilayer is equal with that in directions parallel to the bilayer.[36] The maximum change of the volume of the system in one step has been set to 800 Å^3. The rates of acceptance of the water, overall lipid, and volume-changing moves have resulted in about 1:5, 1:4, and 1:3, respectively. The acceptance rates for the torsional changes ranged between 0.15 and 0.35. The individual values for the 41 torsional angles are summarized elsewhere.[35]

The system has been equilibrated by a 2.3×10^8 Monte Carlo steps long run. After this equilibration period both the energy and the two cellsize parameters (i.e., the hexagon edge and the prism length) have been fluctuating around their equilibrium values. The mean area per headgroup was 57.6 Å^2 which compares reasonably well with the experimental estimate[37] of 59.7 Å^2. In the production phase 1000 sample configurations, separated by 10^5 Monte Carlo moves each, have been saved for the further analyses. The entire simulation required about a 30-week-long run on a single SGI R10000 processor.

To investigate the effect of the lipid membrane on the relative arrangement of the water molecules, we have repeated the performed analyses of the local water structure on pure bulk water as a reference system and have compared the obtained results with those of the different regions of the membrane. For this purpose, we have performed a Monte Carlo simulation of pure TIP3P water on the (*N*, *p*, *T*) ensemble with 512 molecules under similar thermodynamic conditions than in the lipid simulation (i.e., $T = 310$ K, $p = 1$ bar). For the analyses 200 equilibrium configurations, separated by 51 200 moves each, have been saved.

Results and Discussion

Orientation of the Water Molecules Relative to the Lipid Bilayer. The orientation of a water molecule relative to the lipid bilayer can be characterized by the angle α_0 formed by its dipole vector with the bilayer normal vector, which points out of the membrane toward the aqueous phase, and the angle β_0 between

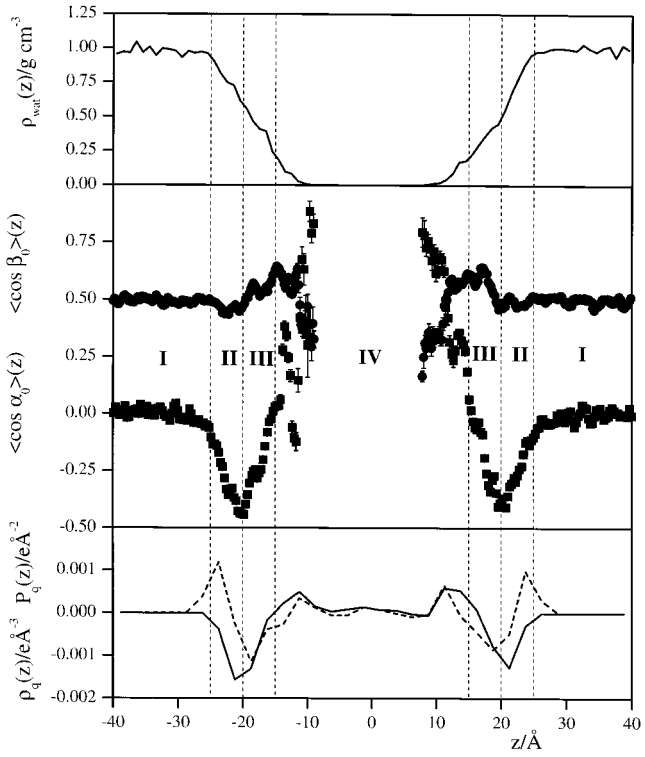

Figure 1. (Top) density profile of water across the DMPC bilayer. (Middle) Average cosine of the angles α_0 between the bilayer normal vector (pointing toward the aqueous phase) and the water dipole moments (full squares), and β_0 formed by the bilayer plane and the plane of the water molecules (full circles) across the DMPC bilayer. Error bars only shown when larger than the symbols themselves. (Bottom) The charge density profile of the lipid molecules $\rho_q(z)$ (dashed line) and its integral with respect to z, $P_q(z)$ (solid line). The dashed vertical lines indicate the partition of the membrane into four different regions for the further analyses.

the plane of the water molecule and the bilayer plane. Figure 1 shows $\langle\cos\alpha_0\rangle(z)$ and $\langle\cos\beta_0\rangle(z)$ along the space-fixed axis perpendicular to the bilayer (denoted here as z). The density profile of water across the membrane $\rho_{wat}(z)$ is also shown. As is seen, beyond ±25 Å the water density is fluctuating around its bulk value, whereas in the interfacial region, between ±25 and ±8 Å it decreases steadily toward the middle of the bilayer. Between -8 and 8 Å (i.e., in the hydrocarbon phase of the membrane) the water density profile is found to be zero in the simulation. The picture obtained is consistent with our previous results on the free energy profile of water across a fully hydrated DMPC bilayer.[25]

The $\langle\cos\alpha_0\rangle(z)$ function, shown on Figure 1, exhibits a much more complex behavior. This profile has already been determined in previous simulations of various phospholipid mono- and bilayers.[17,28,29] The present $\langle\cos\alpha_0\rangle(z)$ function is qualitatively similar to the previous results. In the interfacial region it goes through a minimum around 20 Å and increases rapidly from this minimum toward the middle of the bilayer, becoming positive at about 15 Å. This means that within ±15 Å the water dipoles preferentially turn toward the aqueous phase, whereas between ±15 and ±25 Å their preferential orientation points toward the middle of the membrane. This behavior is the consequence of the fact that the negatively and positively charged groups of the lipid molecules are located at different positions along the z axis.

It should also be noted that the obtained $\langle\cos\alpha_0\rangle(z)$ function is fairly symmetric to the middle of the bilayer. This indicates that its features are not simply resulting from poor statistics, even in the interior of the membrane where only a few water molecules are located. This is also confirmed by the error bars of the calculated $\cos\alpha_0$ values, shown also in Figure 1.

To interpret the behavior of the $\langle\cos\alpha_0\rangle(z)$ function we have also calculated the charge density profile of the lipid molecules along the z axis $\rho_q(z)$, and its integral from the middle of the bilayer toward the aqueous phase $P_q(z)$:

$$P_q(z) = \int_0^z \rho_q(Z)\mathrm{d}Z \qquad (2)$$

The $\rho_q(z)$ and $P_q(z)$ functions are also shown in Figure 1. As is seen, $\rho_q(z)$ goes through a minimum and a maximum at $|z| = 18$ Å and $|z| = 23$ Å, corresponding to the average position of the negatively charged phosphate and the positive tetramethylammonium groups,[38] respectively. Thus, water molecules between ±18 and ±23 Å are located between parallel layers of positive and negative charges, and therefore they turn preferentially toward the negative layer with their dipole moments. However, $\langle\cos\alpha_0\rangle(z)$ is negative in a considerably wider z range, between ±15 and ±25 Å. To fully understand the behavior of $\langle\cos\alpha_0\rangle(z)$, we should focus on the properties of the $P_q(z)$ function. As is seen from Figure 1, the sign of $\langle\cos\alpha_0\rangle(z)$ follows precisely that of $P_q(z)$. Between ±15 and ±25 Å $P_q(z)$ is negative, which means that the water molecules experience here a *net* negative charge density from the middle of the bilayer (and thus, a net positive charge density from the direction of the aqueous phase). Hence, water molecules in this entire z interval are located between a negatively and a positively charged region and are turning toward the negative charges with their dipoles, which makes $\langle\cos\alpha_0\rangle(z) < 0$. However, below ±15 Å $P_q(z)$ becomes positive, indicating that the molecules experience here a net positive charge density from the middle and net negative charge density from the outside of the bilayer. This changes the preferential direction of the water dipoles, turning them toward the outer side of the membrane and making $\langle\cos\alpha_0\rangle(z) > 0$. Similarly, beyond the position of the positive peak of $\rho_q(z)$ at ±23 Å the $P_q(z)$ function is still negative. Hence, water dipoles turn here preferentially toward the net negative charge density in the membrane interior. This preference vanishes around ±25 Å, where $P_q(z)$ damps also to zero.

According to the behavior of the $\langle\cos\alpha_0\rangle(z)$ function we divide the membrane into four regions and perform the following analyses on the individual regions separately. Region I at $|z| \geq 25$ Å is the bulk water region, where $\rho_{wat}(z)$ reaches the bulk water density and $\langle\cos\alpha_0\rangle(z)$ fluctuates around zero. Region II, between ±20 and ±25 Å covers the z range in which $\langle\cos\alpha_0\rangle(z)$ decreases with decreasing $|z|$. In region III, at $15\ \text{Å} \leq |z| < 20$ Å, $\langle\cos\alpha_0\rangle(z)$ is still negative, but it increases toward the middle of the bilayer and becomes positive below ±15 Å, in region IV. The definition of the four regions is also shown in Figure 1, whereas Table 1 summarizes the average values of the calculated quantities in the individual regions of the bilayer. It should be emphasized that this division of the membrane into separate regions is made in a different way than that of Marrink and Berendsen,[12] and thus the properties of the individual regions can also be different from theirs.

The behavior of $\langle\cos\beta_0\rangle(z)$ is considerably simpler than that of $\langle\cos\alpha_0\rangle(z)$. Since β_0 is the angle of two planes (i.e., the plane of the water molecule of interest and the lipid bilayer), it can only vary between 0 and 90°, and thus $\cos\beta_0$ is in the range of $0 \leq \cos\beta_0 \leq 1$. If the water molecules have no preferential alignment relative to the bilayer plane, then $\langle\cos\beta_0\rangle$ is 0.5, whereas $\langle\cos\beta_0\rangle < 0.5$ and $\langle\cos\beta_0\rangle > 0.5$ indicates preferential

TABLE 1: Average Density and Orientational Properties of Water in the Different Regions of the Membrane

region	(|z| range)/Å	$\langle\rho_{wat}\rangle$/g cm^{-3}	$\langle\cos\alpha_0\rangle$	$\langle\cos\beta_0\rangle$	$\langle\cos\alpha\rangle$	$\langle\cos\beta\rangle$	$\langle\cos\gamma\rangle$	$\langle\cos\theta\rangle$
I	40−25	0.986	−0.010	0.496	0.410	0.502	0.956	−0.194
II	25−20	0.762	−0.254	0.476	0.445	0.512	0.942	−0.189
III	20−15	0.381	−0.233	0.546	0.441	0.525	0.943	−0.185
IV	15−0	0.089	0.232	0.575	0.451	0.521	0.940	−0.165

perpendicular and parallel orientation of the molecules relative to the bilayer plane, respectively. As is seen from Figure 1, $\langle\cos\beta_0\rangle(z)$ fluctuates around 0.5 in regions I and II (with a very slight preference of perpendicular alignment in region II). In region III $\langle\cos\beta_0\rangle(z)$ becomes larger than 0.5, and this preferential parallel alignment persists until about $|z| = 11.5$ Å. Below 11.5 Å $\langle\cos\beta_0\rangle$ decreases sharply, indicating that the few water molecules which penetrate deeply, up to about ±8 to ±10 Å, into the membrane prefer to be aligned perpendicular to the plane of the bilayer. Since these molecules are located between the hydrocarbon chains of the lipid molecules, this preference can be explained by (i) the fact that in an apolar environment of rather low water density the effect of the electric field of the zwitterionic headgroups is not perturbed by the field of the other water molecules, and (ii) the effect of the hydrocarbon chains, which are perpendicular to the bilayer plane and force the water molecules to be aligned parallel with them.

In the above analysis we assumed that the $P(\cos\alpha_0)$ and $P(\cos\beta_0)$ distributions are monotonic in every layer of the membrane. Although this assumption is certainly sensible, in principle it is not necessarily true. For instance, we interpreted $\langle\cos\alpha_0\rangle \approx 0$ in region I as an indication of the lack of any orientational preference of the water molecules relative to the bilayer normal. However, in principle it can also be the consequence of preferential perpendicular alignment as well as equally strong parallel and antiparallel preferences, etc. Similarly, $\langle\cos\alpha_0\rangle > 0$ or $\langle\cos\alpha_0\rangle < 0$ does not necessarily mean simply that the water dipoles are pointing preferentially out of the membrane or toward the middle of the bilayer, respectively, but can also be the consequence of various kinds of complex dipole orientation preferences. To demonstrate that the above assumption is indeed true in our case, we have calculated the probability density of both $\cos\alpha_0$ and $\cos\beta_0$ in the four regions separately. The resulting $P(\cos\alpha_0)$ and $P(\cos\beta_0)$ distributions are shown in Figure 2. As is evident, all distributions are indeed either uniform or changing monotonically. Both $P(\cos\alpha_0)$ and $P(\cos\beta_0)$ are uniform in region I, $P(\cos\alpha_0)$ decreases monotonically in regions II and III (i.e., where $\langle\cos\alpha_0\rangle(z)$ is negative) and increases in region IV where $\langle\cos\alpha_0\rangle(z) > 0$. Thus, the water dipoles are indeed pointing toward the middle of the membrane preferentially in regions II and III and toward the aqueous phase in region IV (i.e., the maximum position of the corresponding $P(\cos\alpha_0)$ functions are at −1 and 1, respectively). Similarly, $P(\cos\beta_0)$ shows a slight preference for perpendicular alignment in region II and a considerably stronger parallel preference in regions III and IV. It should be noted that although this preferential parallel alignment in region IV is in agreement with the fact that $\langle\cos\beta_0\rangle(z)$ is somewhat larger than 0.5 between ±11.5 and ±15 Å, it seems to be contradicted by the sharp decrease of $\langle\cos\beta_0\rangle(z)$ below ±11.5 Å. However, below ±11.5 Å the number of the water molecules is very low (see the water density profile curve in Figure 1), and therefore the relative importance of their orientational preference is very small compared to that of the much larger number of water molecules between ±11.5 and ±15 Å in this region.

Pair Distribution Functions. The change of the water structure on the level of two-particle correlations can simply be monitored along the DMPC bilayer by calculating the $g_{ij}(r)$

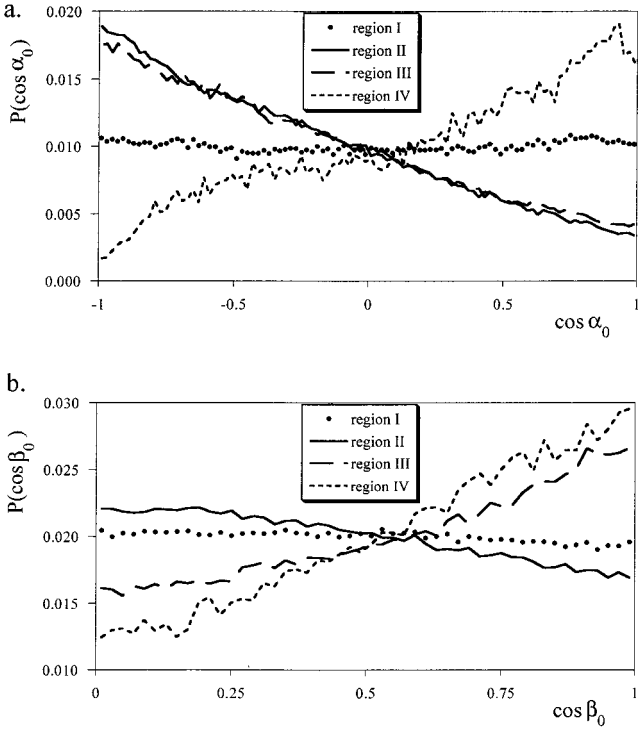

Figure 2. (a) Cosine distribution of the α_0 angle formed by the bilayer normal vector (pointing toward the aqueous phase) with the dipole moment of the individual water molecules in the four different regions of the DMPC membrane. (b) Cosine distribution of the β_0 angle between the bilayer plane and the plane of the individual water molecules in the four different regions of the DMPC membrane.

partial pair correlation functions in the different membrane regions. However, since $g_{ij}(r)$ is defined as $g_{ij}(r) = \rho_{ij}(r)/\rho_j$, where $\rho_{ij}(r)$ is the density of the j type atoms at a distance r from the central atom of type i and ρ_j is the average density of the j type atoms in the entire system; and because of the water molecules are distributed rather inhomogeneously in the membrane (see Figure 1), the resulting partial pair correlation functions are reflecting not only the differences of the two-body structure but also that of the average density of water in the different membrane regions. Therefore, instead of the ordinary $g_{ij}(r)$ partial pair correlation functions we have calculated the $g'_{ij}(r)$ functions, in which the $\rho_{ij}(r)$ density is normalized by $\langle\rho_j\rangle_{reg}$, the average density of the atoms of type j in the region of interest:

$$g'_{ij}(r) = \frac{\rho_{ij}(r)}{\langle\rho_j\rangle_{reg}} = g_{ij}(r)\frac{\rho_j}{\langle\rho_j\rangle_{reg}} \tag{3}$$

Obviously, in pure water $g'_{ij}(r)$ becomes identical with $g_{ij}(r)$. The $g'_{ij}(r)$ functions obtained are presented in Figure 3a in the four different membrane regions and in pure water. The running coordination numbers $c_{ij}(r)$, related to $g'_{ij}(r)$ through the equation

$$c_{ij}(r) = 4\pi\langle\rho_j\rangle_{reg}\int_0^r R^2 g'_{ij}(R)\mathrm{d}R \tag{4}$$

are plotted in Figure 3b.

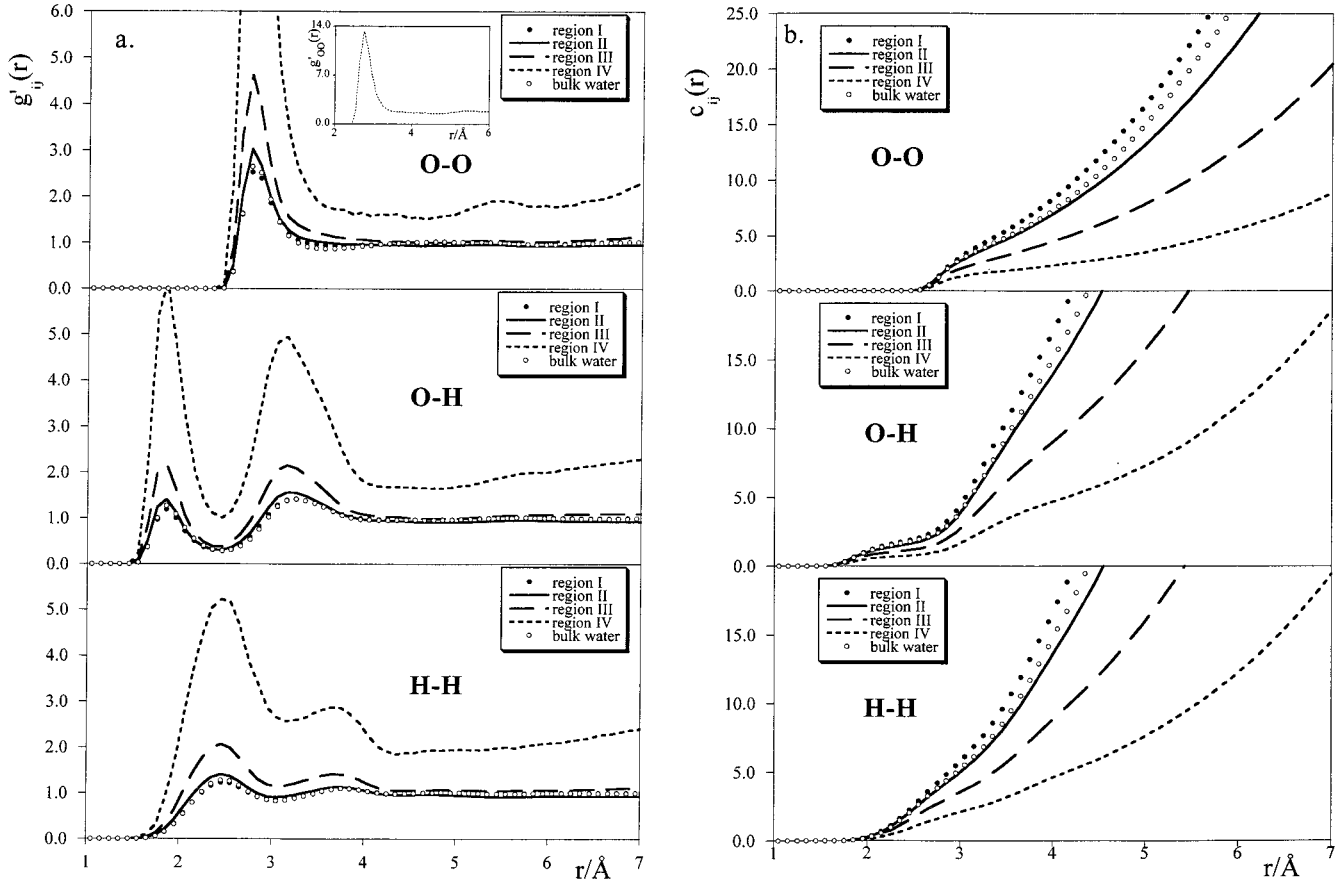

Figure 3. (a) Partial pair correlation functions of water in the four different regions of the DMPC membrane and in pure water. The pair correlation functions are normalized by the average density of water in the region of interest instead of that in the entire system (see text). The inset shows the $g'_{OO}(r)$ function of region IV on a different scale. (b) Running coordination numbers of water in the four different regions of the DMPC membrane and in pure water.

As it can be seen, the $g'_{ij}(r)$ functions in region I and II are very similar to those of bulk water, indicating that the two-body structure of water does not change noticeably from the bulk phase to region II. All three $g'_{ij}(r)$ functions are damping to 1 at large r values, indicating that despite the overall decrease of the water density toward the bilayer center in region II, the local density within 7 Å around the molecules appears to be almost homogeneous even in this region. Although the three $g'_{ij}(r)$ functions are still damping to values close to 1 in region III, they are always above the corresponding bulk water functions up to 7 Å. This is a sign of the inhomogeneity of the water density in this region. Besides this difference, the $g'_{ij}(r)$ functions are still rather similar to those in bulk water, the peaks and minima appear at the same positions indicating that the relative arrangement of the hydrogen-bonded neighbors, and thus the geometry of the hydrogen bonds does not change considerably from bulk water to region III. However, despite the general agreement, there is also a notable difference between the two sets of functions. This difference appears on the $g'_{OO}(r)$ functions between about 3 and 4 Å, after the first, hydrogen-bonding peak. Here $g'_{OO}(r)$ decreases considerably less rapidly in region III than in bulk water. This r range is typical of the distance of the interstitial water neighbors, which have left the tetrahedral hydrogen-bonded network of the other molecules and are located in its cavities.[3−6] Hence, this difference of the $g'_{OO}(r)$ functions indicates that the relative importance of the interstitial molecules in the local structure of water is larger in region III than in pure water.

In region IV the situation is rather different from that in the outer regions. Here the $g'_{ij}(r)$ functions are always much higher than in the other regions, and they are not even approaching 1 up to 7 Å. This is a clear indication of the presence of large density fluctuations even on a small r scale here. The position of the first peaks and minima of all three functions are still the same here as they are in pure water. However, the heights of these peaks are very large, the first peak is about 4.5 times higher here than in pure water for all three functions. In contrast to the peak heights, the ratio of the $g'_{ij}(r)$ functions of the two systems in their relatively flat part, between 5 and 7 Å, is only about 2. Moreover, the c_{OO} coordination number value at 3.3 Å as well as that of c_{OH} at 2.5 Å reveals that in region IV the number of the hydrogen-bonded neighbors of the molecules is about 1.6, that is, about 40% of that in bulk water, whereas the average water density in this region is less than 10% of the bulk water value (see Table 1). This means that the few water molecules present in this region are still forming hydrogen-bonded clusters, and thus they cannot fill this region uniformly. The fact that the molecules have about 1.6 hydrogen-bonded neighbors on average suggests that these hydrogen-bonded clusters are probably predominantly short chainlike structures.

Relative Orientation of the Neighboring Water Molecules. In this section the relative orientation of the neighboring water molecules is analyzed in each of the four regions of the DMPC bilayer. Two molecules are regarded here as "neighbors" if their O−O distance is smaller than 3.3 Å, the first minimum position of the $g_{OO}(r)$ function in bulk water. The relative orientation of the neighboring molecules is characterized by their dipole−dipole and plane−plane angles (α and β, respectively), whereas the geometry of their hydrogen bonds is described by the γ angle around the hydrogen donor O atom (H−O···O angle) and

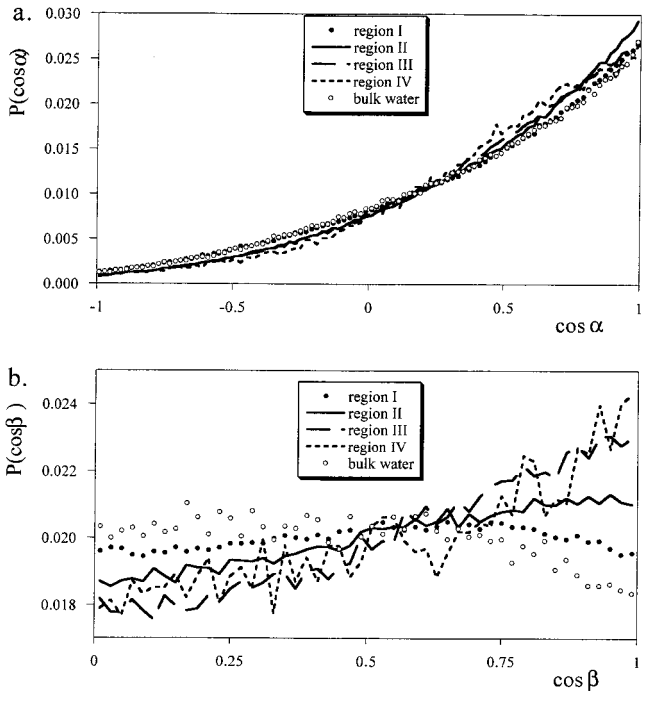

Figure 4. (a) Cosine distribution of the α angle formed by the dipole moments of two neighboring water molecules in the four different regions of the DMPC membrane and in pure water. (b) Cosine distribution of the β angle between the planes of two neighboring water molecules in the four different regions of the DMPC membrane and in pure water.

by the θ angle formed by the O atoms of two neighbor molecules around the O atom of the central molecule (O···O···O angle).

The cosine distributions of the angles describing relative orientation of the molecules, $P(\cos\alpha)$ and $P(\cos\beta)$, are shown in Figure 4. Although, due to the poor statistics available in region IV, the resulting functions are considerably noisier there than in the outer membrane regions, the main features of these functions are not affected by this noise. It is seen that the lipid bilayer shows little influence on the $P(\cos\alpha)$ distribution, which is very similar to that of bulk water in all four membrane regions. In particular, the curve obtained in region I is almost identical to that of pure TIP3P water. In the three regions located in the membrane interface the $P(\cos\alpha)$ function is somewhat larger for $\cos\alpha > 0$ (i.e., $\alpha < 90°$) and smaller for $\cos\alpha < 0$ than in bulk water, indicating that the preference of the neighboring water molecules for parallel dipole−dipole orientation is slightly stronger in the membrane than in the bulk phase. This is also demonstrated by the average values of $\cos\alpha$ in the different regions, collected in Table 1. A similar effect is observed for the preferential arrangement of the molecular planes. As is seen in Figure 4b, the deeper the neighboring water molecules penetrate into the membrane the stronger is their preference for a parallel plane−plane alignment. In pure water the $P(\cos\beta)$ distribution is roughly uniform between 0 and 0.6 and decreases from 0.6 to 1, indicating that no specific preference is given to any angle between about 55° and 90°; however, angles below 55° are not preferred. The shape of $P(\cos\beta)$ in region I is still similar to that of bulk water; it is uniform below 0.6 and decreases from 0.6 to 1, but the steepness of this decrease is considerably smaller than in pure water. However, in regions II−IV $P(\cos\beta)$ increases monotonically, with a greater steepness in the regions closer to the middle of the membrane, in the entire [0,1] interval.

The increasing preference of the neighboring molecules observed for both parallel dipole−dipole and plane−plane alignment with their increasing penetration into the bilayer is a consequence of the ordering effect of the membrane on the orientation of the water molecules, which has been discussed in the previous section and demonstrated in Figure 1. Namely, in regions II−IV there are specific directions (i.e., the middle of the membrane in regions II and III, and the aqueous phase in region IV) toward which the water dipoles are preferentially pointing. Therefore, the dipoles of the neighboring molecules prefer to point in the same direction, which increases also their preference for parallel dipole−dipole alignment. This ordering effect is negligible in region I (i.e., here $\langle\cos\alpha_0\rangle$ is almost zero and $P(\cos\alpha_0)$ is roughly uniform, as seen from Table 1 and Figure 2a) and is roughly equally strong in regions II−IV (i.e., the deviation of $\langle\cos\alpha_0\rangle$ from zero and the magnitude of the steepness of $P(\cos\alpha_0)$ are roughly equal in these three regions). This can explain the facts that (i) the $P(\cos\alpha)$ distribution in region I deviates negligibly from that in bulk water, and (ii) the $P(\cos\alpha)$ distributions are almost identical in regions II−IV.

Similarly, the membrane has no ordering effect on the orientation of the water planes in region I, but such effect can be observed in region II and in a considerably stronger form in regions III and IV (see the $\langle\cos\beta_0\rangle$ values in Table 1 and the $P(\cos\beta_0)$ distributions in Figure 2b). This is again consistent with the increasing preference of the neighbors for parallel plane−plane alignment with their increasing penetration into the membrane, as shown in Figure 4b.

The $P(\cos\beta_0)$ distributions observed can also provide some information on the distortion of the hydrogen-bonding structure around the water molecules in the different regions of the bilayer. Assuming tetrahedral arrangement of the hydrogen-bonded neighbors and linear hydrogen bonds (i.e., $\theta = 109.5°$ and $\gamma = 0°$), the β angle can only vary between about 55° and 90°. Therefore, the deviation of the observed $P(\cos\beta)$ curves from 0 above 0.57 is an indication for the deviation of the hydrogen-bond geometries present in the system from these assumptions. Namely, the relative arrangement of the pairs with large $\cos\beta$ values must strongly deviate from linear hydrogen bonds and tetrahedral nearest-neighbor arrangement. These pairs are likely containing interstitial water molecules, which can easily be as close to their network-forming neighbors as real hydrogen-bonding pairs; however, they usually do not form strong hydrogen bonds with them. The fact that in pure water $P(\cos\beta)$ decreases steadily above 0.6 indicates that although the above assumptions are not fully satisfied, they describe an approximate geometry of the hydrogen bonds here. On the other hand, the increasing fraction of neighbors having large $\cos\beta$ values with their increasing penetration into the bilayer indicates that the closer the water neighbors are to the middle of the membrane the stronger is the deviation of their relative arrangement from the optimal geometry for the hydrogen-bonded pairs.

To analyze this point further we have separately investigated the fulfillment of these two assumptions in the different membrane regions and in pure water. For this purpose, we have also calculated the cosine distribution of the H−O···O angle of the hydrogen bonds, γ, and that of the θ angle formed by two neighbors around the central molecule. In calculating the $P(\cos\gamma)$ distributions we took into account only those neighbors that had an O···H pair closer than 2.5 Å, the first minimum position of the $g_{OH}(r)$ partial pair correlation function, with the central molecule. The resulting distributions are shown in Figure

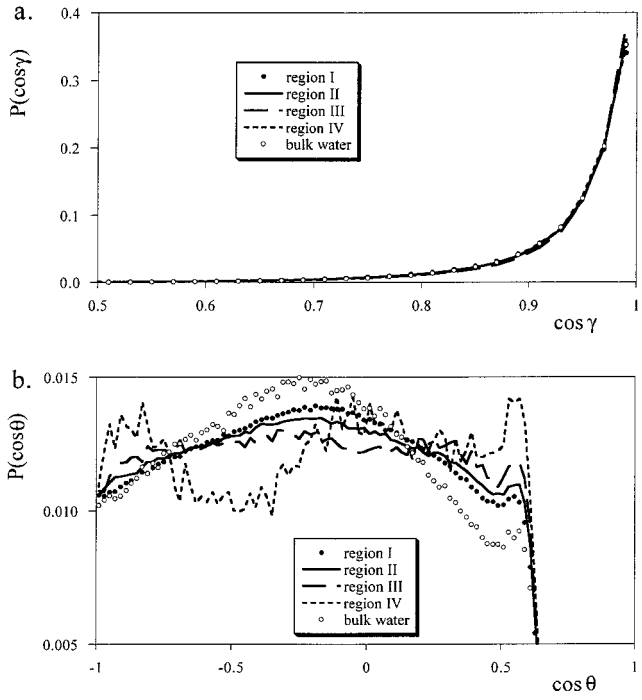

Figure 5. (a) Cosine distribution of the H−O···O hydrogen-bond angle γ in the four different regions of the DMPC membrane and in pure water. (b) Cosine distribution of the angle θ formed by the O atoms of two neighbor molecules around the O atom of the central molecule (O···O···O angle) in the four different regions of the DMPC membrane and in pure water.

5. As is clearly seen, the $P(\cos\gamma)$ distributions are practically identical in all four different membrane regions and also in pure water. The distributions have a high peak at 1, corresponding to linear hydrogen bonds, and they damp to zero around 0.7 (i.e., at $\gamma = 45°$). The strength of this preference of the hydrogen bonds for linear geometry can be demonstrated by integrating the $P(\cos\gamma)$ distributions, which reveals that $\gamma < 15°$ in 55% and $\gamma < 30°$ in 90% of the hydrogen bonds.

Contrary to γ, the cosine distribution of the O···O···O angle changes dramatically upon going from bulk water toward the hydrocarbon phase of the membrane. In pure water $P(\cos\theta)$ is a bimodal distribution, having a large, broad peak around −0.3 and a small but clear peak at 0.5. The former peak is formed by the tetrahedrally arranged neighbors, whereas the latter one is a sign of the interstitial molecules. The position of this peak indicates that around the interstitial molecules the neighbors are arranged in a closely packed way as they form equilateral triangles. This peak is roughly as much higher than the preceding minimum in pure water than in regions I and II of the membrane. However, this difference of the height of this peak and the preceding minimum becomes more than twice as high in region III and about 5 times higher in region IV, indicating that the relative importance of the closely packed structural units increases toward the middle of the membrane.

On the other hand, the tetrahedral peak of the $P(\cos\theta)$ distribution is lower and broader, and thus the entire distribution function is less structured in the bulk water region of the DMPC membrane than in pure water. In region II this peak becomes even lower and broader, whereas in region III it disappears completely and the distribution becomes practically uniform between −1 and 0.4. This means that the preference of the hydrogen-bonded neighbors for being arranged in tetrahedral directions around the central molecule becomes weaker when moving from bulk water toward the middle of the DMPC membrane, and it is already lost in region III. This is very similar to what happens in pure water with increasing temperature and decreasing density.[39,40] However, in region IV the $P(\cos\theta)$ distribution becomes again well structured, although this structure is now completely different from that in bulk water. Besides the close-packed peak at 0.5, there is a peak around 0 and another one slightly above −1. This distribution reflects planar preferential arrangement of the neighbors around the central molecule. In such an arrangement the hydrogen donor neighbor molecule is located in the plane of the central molecule in a direction perpendicular to one of its O−H bonds (i.e., to the direction of one of its hydrogen acceptor neighbors). The angle between this direction and the other O−H bond of the central molecule is about 165°, corresponding to the $\cos\theta$ value of −0.96 where the other peak of $P(\cos\theta)$ is located. Similar to the preference for the parallel plane−plane orientation of the neighbor molecules in region IV, this preference for their coplanar spatial arrangement is also a consequence of the constraints imposed by the hydrocarbon lipid chains, which force the water molecules as well as their hydrogen bonds to be aligned in planes parallel with them.

Spherical Harmonic Expansion of the Orientational Pair Correlation Function. The relative arrangement of the molecular pairs in a system can fully be characterized by their $g(r,\omega_1,\omega_2,\omega)$ orientational pair correlation function. Among the arguments of the orientational pair correlation function $\omega_1 = (\phi_1,\vartheta_1,\chi_1)$ and $\omega_2 = (\phi_2,\vartheta_1,\chi_2)$ are the Euler angles describing the orientation of the two molecules in a space-fixed coordinate system, whereas r and $\omega = (\vartheta,\phi)$ are the polar coordinates of the vector joining the two molecular centers in this frame. However, among the nine variables of $g(r,\omega_1,\omega_2,\omega)$ only six are independent, and thus, with an appropriate choice of the reference frame, three of them can be eliminated. Such an appropriate choice is to fix the origin at the position of the center of the first molecule and the z axis along the vector joining the two molecular centers. In this frame ω is eliminated, and instead of ϕ_1 and ϕ_2 their difference $\Delta\phi = \phi_2 - \phi_1$ is independent. The orientational pair correlation function can be expanded in this frame into a series as[41,42]

$$g(r,\omega_1,\omega_2) = \sum_{l_1 l_2 l} \sum_{n_1 n_2} g_{l_1 l_2 l, n_1 n_2}(r)\Phi_{l_1 l_2 l, n_1 n_2}(\omega_1,\omega_2) \qquad (5)$$

The range of the indices in this summation is restricted to $l_1 \geq 0$, $l_2 \geq 0$, and $(l_1 + l_2) \geq l \geq |l_1 - l_2|$. This expansion separates the distance and orientation dependence of the orientational pair correlation function. The $g_{l_1 l_2 l, n_1 n_2}(r)$ coefficients of the expansion depend only on the center−center distance, whereas the $\Phi_{l_1 l_2 l, n_1 n_2}(\omega_1,\omega_2)$ basis functions only on the relative orientation of the molecules. $\Phi_{l_1 l_2 l, n_1 n_2}(\omega_1,\omega_2)$ can be written as

$$\Phi_{l_1 l_2 l, n_1 n_2}(\omega_1,\omega_2) = \sum_{m=-l_0}^{l_0} C(l_1 l_2 l, m\underline{m}0) D^{l_1 *}_{m n_1}(\omega_1) D^{l_2 *}_{\underline{m} n_2}(\omega_2) \qquad (6)$$

where $l_0 = \min(l_1, l_2)$, $\underline{m} = -m$, $C(l_1 l_2 l, m\underline{m}0)$ are the Clebsch−Gordan coefficients, $D^l_{mn}(\omega)$ is the generalized spherical harmonic function of order mnl,[42] and * denotes complex conjugate. Using the sum rules of the Clebsch−Gordan coefficients and the orthogonality of the $D^l_{mn}(\omega)$ functions,[42] equation 5 can be inverted, and the expansion coefficients can be expressed as

$$g_{l_1 l_2 l, n_1 n_2}(r) = (2l_1 + 1)(2l_2 + 1) g_{cc}(r) \langle \Phi^*_{l_1 l_2 l, n_1 n_2}(\omega_1,\omega_2) \rangle_r \qquad (7)$$

where $g_{cc}(r)$ is the center-center pair correlation function of the

molecules, and the brackets $\langle\cdots\rangle_r$ denote ensemble averaging over the orientation of all pairs of molecules separated by the center-center distance of r. Thus, the $g_{000,00}(r)$ coefficient is identical with $g_{cc}(r)$. It should be noted that the coefficients in this formalism differ by a factor of $[(2l+1)/4\pi]^{1/2}$ from those of Gray and Gubbins,[42] where $g_{000,00}(r) = \sqrt{4\pi}g_{cc}(r)$.

The $g_{000,00}(r)$ coefficients obtained in the different membrane regions and in pure water are shown in Figure 6. Since these functions are the partial pair correlation functions of the water center-of-masses, they are rather similar to the $g_{OO}(r)$ partial pair correlation functions, although there are also some differences between them. The most important of these differences is the presence of a broad and low but clear second peak around 4.5 Å on the $g_{000,00}(r)$ function of pure water. This second peak of $g_{000,00}(r)$, reflecting the second neighbors of the molecules in the tetrahedral network, is also present in the bulk water-like region I of the membrane, but it disappears in the inner membrane regions where the tetrahedral orientation of the hydrogen-bonded neighbors becomes weaker.

While $g_{000,00}(r)$ only describes the radial distribution of the molecular center-of-masses, the higher-order coefficients represent real orientational correlation between the molecules. Four of these coefficients are shown in Figure 7a. The amplitude of the peaks of the $g_{l_1l_2l,n_1n_2}(r)$ coefficients can usually provide information on the strength of the orientational correlation of the molecules. However, due to their proportionality with the center−center pair correlation function $g_{cc}(r)$, in the case of our inhomogeneous system they also reflect the density of the water molecules in the given membrane region (see eqs 3 and 7). Indeed, the order of the first peak height of $g_{000,00}(r)$ agrees, with a few exceptions, with that of the amplitude of the first extremum of the higher−order coefficients (see Figures 6 and 7a). Therefore, the calculation of the orientational average of the angle-dependent basis functions of the expansion of eq 5, $\langle\Phi_{l_1l_2l,n_1n_2}(\omega_1,\omega_2)\rangle_r$, can also be rather informative in our case. The obtained $\langle\Phi_{l_1l_2l,n_1n_2}(\omega_1,\omega_2)\rangle_r$ functions corresponding to the coefficients shown in Figure 7a are plotted in Figure 7b. These functions can be expressed in explicit form as

$$\langle\Phi_{101,00}(\omega_1,\omega_2)\rangle r = \langle\cos\vartheta_1\rangle_r$$

$$\langle\Phi_{110,00}(\omega_1,\omega_2)\rangle r = -\frac{1}{\sqrt{3}}\langle\cos\alpha\rangle_r$$

$$\langle\Phi_{112,00}(\omega_1,\omega_2)\rangle r = -\frac{1}{\sqrt{2}\sqrt{3}}\langle\cos\alpha - 3\cos\vartheta_1\cos\vartheta_2\rangle_r \quad (8)$$

$$\langle\Phi_{211,00}(\omega_1,\omega_2)\rangle r = -\frac{1}{2\sqrt{5}}\langle(3\cos^2\vartheta_1 - 1)\cos\vartheta_2 + 3\sin\vartheta_1\cos\vartheta_1\sin\vartheta_2\cos\phi\rangle_r$$

where α is the dipole−dipole angle of the two molecules.

As is seen from Figure 7a, the sign and shape of the $g_{l_1l_2l,n_1n_2}(r)$ coefficients, with the exception of the $g_{101,00}(r)$ function of region IV, agree well in the different membrane regions and in pure water, indicating that the main orientational preferences of the water pairs persist from the bulk phase to the inner membrane regions. On the other hand, the comparison of the $\langle\Phi_{l_1l_2l,n_1n_2}(\omega_1,\omega_2)\rangle_r$ functions can also reveal the changes in the details of these main orientational preferences. As is seen from Figure 7b, the $\langle\Phi_{l_1l_2l,n_1n_2}(\omega_1,\omega_2)\rangle_r$ functions of regions I and II agree very well with those of bulk water within the first coordination shell of the molecules. At larger distances, this agreement is still very good in region I, and the shape of the $\langle\Phi_{l_1l_2l,n_1n_2}(\omega_1,\omega_2)\rangle_r$ functions of regions II and III are also rather

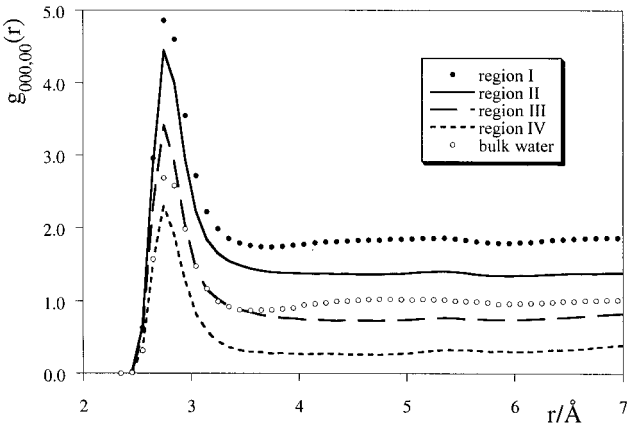

Figure 6. $g_{000,00}(r)$ coefficient of the spherical harmonic expansion of the orientational pair correlation function of water in the four different regions of the DMPC membrane and in pure water.

similar to the results of pure water. Such general similarity can also be found between the $\langle\Phi_{110,00}(\omega_1,\omega_2)\rangle_r$ and $\langle\Phi_{112,00}(\omega_1,\omega_2)\rangle_r$ functions of region IV and bulk water. However, the $\langle\Phi_{101,00}(\omega_1,\omega_2)\rangle_r$ and $\langle\Phi_{211,00}(\omega_1,\omega_2)\rangle_r$ functions (i.e., the ones which do not depend on the relative dipole−dipole orientation of the two molecules) of region IV differ from those of pure water in several features. Thus, the first minimum of $\langle\Phi_{101,00}(\omega_1,\omega_2)\rangle_r$ at 2.75 Å is missing in region IV, where this function does not even go below zero. On the other hand, it has a much larger maximum at about 3.2 Å here than in the outer regions or in pure water. These differences of the $\langle\Phi_{101,00}(\omega_1,\omega_2)\rangle_r$ functions of the different membrane regions are consistent with our previous findings. As seen from eq 8, this function can simply be written as $\langle\cos\vartheta_1\rangle_r$, where ϑ_1 is the angle formed by the dipole vector of molecule 1 and the vector pointing from the center of molecule 1 to that of molecule 2. Considering a hydrogen-bonding pair with a linear hydrogen bond (i.e., $\gamma = 0$) and neglecting the difference between the position of the O atom and center-of-mass of the molecules, the value of ϑ_1 is 52.26° (i.e., the half of the H−O−H bond angle), corresponding to $\cos\vartheta_1 = 0.61$, in cases when molecule 1 is the H donor in the hydrogen bond. In that case when molecule 1 is the H acceptor, $\cos\vartheta_1 = -0.52$ if the O−O vector forms tetrahedral angles with the O−H bonds of molecule 1, whereas it becomes smaller if the O−O vector direction moves between the two (tetrahedral) directions from which hydrogens can be accepted (i.e., toward the direction opposite to the bisector of the H−O−H bond angle), and becomes larger if the O−O vector moves toward the H atoms of molecule 1. Thus, the fact that the first minimum of $\langle\Phi_{101,00}(\omega_1,\omega_2)\rangle_r$ becomes deeper in region III than in the outer regions reflects the breakdown of the tetrahedral arrangement of the nearest neighbor molecules. On the other hand, the increase of the function here and also around the first maximum at 3.2 Å in region IV indicates the increasing importance of the neighbors located in interstitial directions. Both effects have also been discussed in the previous section and demonstrated in Figure 5b.

The interpretation of the $g_{110,00}(r)$ and $\langle\Phi_{110,00}(\omega_1,\omega_2)\rangle_r$ functions is rather straightforward, since they are both proportional to $-\langle\cos\alpha\rangle_r$. The negative sign of the main extremum of the $g_{110,00}(r)$ functions in every region is consistent with our previous finding of preferential parallel dipole−dipole arrangement of the neighbor water molecules all across the membrane. The fact that all five $\langle\Phi_{110,00}(\omega_1,\omega_2)\rangle_r$ functions agree very well with each other below 3.3 Å is again consistent with the previous result that the $P(\cos\alpha)$ distributions of the neighbors are rather

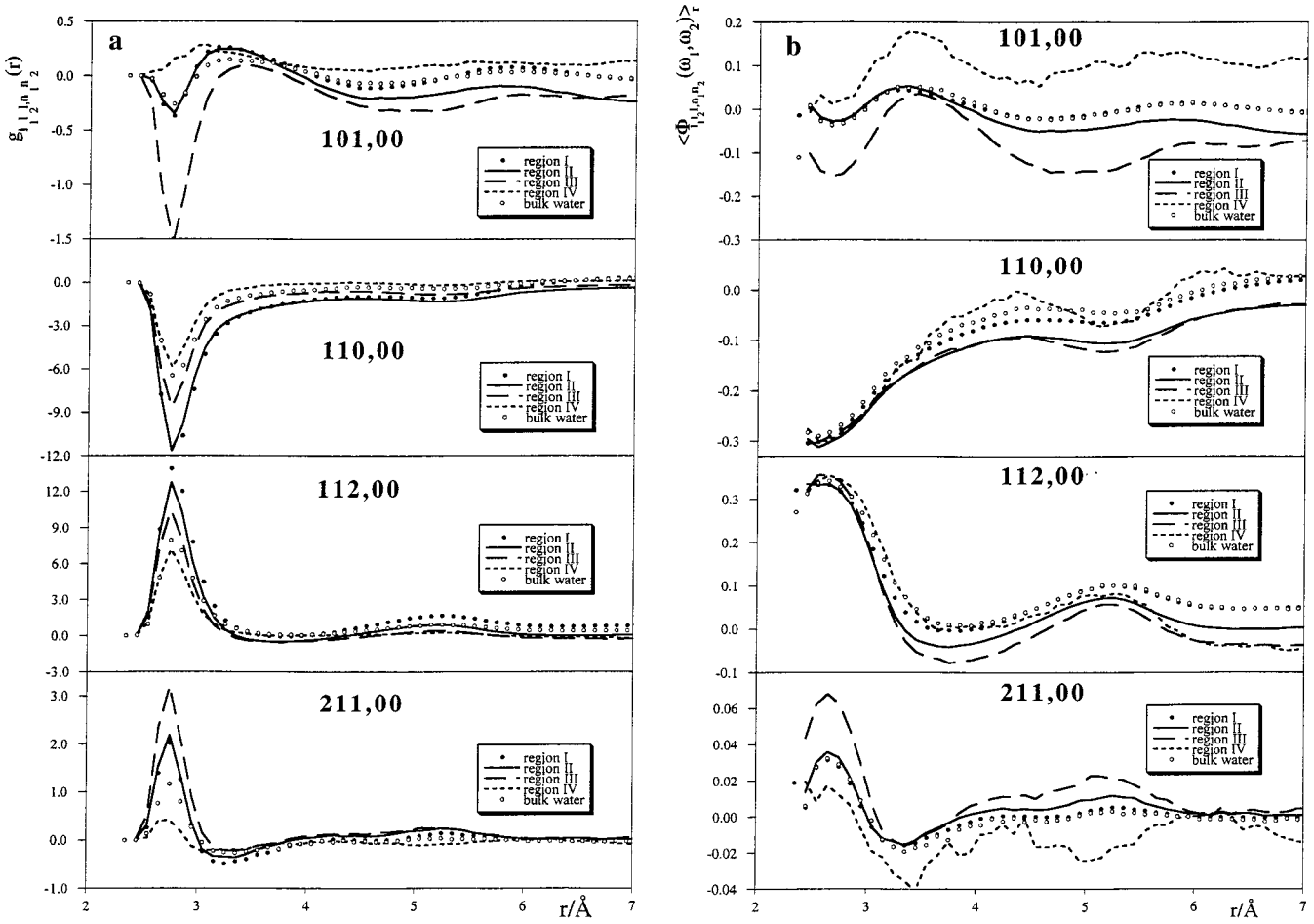

Figure 7. (a) Higher order $g_{l_1l_2l,n_1n_2}(r)$ coefficients of the spherical harmonic expansion of the orientational pair correlation function of water in the four different regions of the DMPC membrane and in pure water. (b) Orientational average of the angle dependent $\Phi_{l_1l_2l,n_1n_2}(\omega_1,\omega_2)$ basis functions of the spherical harmonic expansion of the orientational pair correlation function of water for pairs separated by the distance of r in the four different regions of the DMPC membrane and in pure water.

similar in the different membrane regions (see Figure 4a). It is also seen that above 3.3 Å the $\langle\Phi_{110,00}(\omega_1,\omega_2)\rangle_r$ function in regions II and III is considerably lower than that in bulk water or in region I. This is the consequence of the ordering effect of the membrane on the water dipoles in these regions (see Figures 1 and 2a and also the $\langle\cos\alpha\rangle$ values in Table 1). Although the membrane has a similarly strong ordering effect on the water dipoles in region IV, here the preferential direction of the water dipoles is the opposite as in the neighboring region III. Thus, the relatively few water molecules of region IV have numerous neighbors of opposite dipole orientation beyond 4 Å in region III. These pairs are responsible for the fact that despite the ordering effect of the membrane the $\langle\Phi_{110,00}(\omega_1,\omega_2)\rangle_r$ function is even larger in region IV than in bulk water beyond 4 Å.

Summary and Conclusions

We have discussed the changes in the orientation of the water molecules from the bulk phase to the hydrocarbon region of a DMPC membrane in detail. Most of these changes are related to the change of the electrostatic field along the bilayer normal. Namely, the cumulative charge distribution $P_q(z)$ determines the preferential direction of the water dipoles all across the membrane, and thus it influences also the relative orientation of the neighbor molecules.

In determining the water orientation in the inner region of the membrane the effect of the long lipid tails, which are generally perpendicular to the membrane−water interface, becomes an important factor. These tails force the water molecules into planes parallel to them. This effect is enhanced by the fact that the lack of a substantial number of polar neighbors in this region increases the importance of the electric field of the zwitterionic headgroups in the ordering of the molecular dipole vectors. As a consequence, in this region (i) the plane of the water molecules is preferentially perpendicular to the interface, and (ii) the neighboring molecules prefer to be aligned in parallel planes. For similar reasons, the hydrogen-bonded neighbors are also arranged preferentially in a coplanar manner around the central molecule here.

In analyzing the hydrogen-bonding structure of the water molecules it is found that upon approaching the membrane interior, simultaneously with the decrease of the water density, interstitial molecules play a more important role in the local structure, whereas the preference of the hydrogen-bonded neighbors for being arranged tetrahedrally around the central molecule becomes weaker and vanishes completely in the interfacial region. The preference of the hydrogen bonds themselves for a linear geometry, on the other hand, does not change noticeably from bulk water to the hydrocarbon phase of the membrane. These findings are in a qualitative agreement with the changes observed in the hydrogen-bonding structure of pure water, when the density of the system is decreasing due to the changing thermodynamic conditions.[39] This remarkable agreement emphasizes the strong relation between the peculiar tetrahedral structure and the density of water, which is

also responsible for the anomalous thermodynamic properties, such as the density maximum at 277 K, of liquid water.[6]

Acknowledgment. P.J. is an Eötvös Fellow of the Hungarian Ministry of Culture and Education, which is gratefully acknowledged.

References and Notes

(1) Eisenberg, D. S.; Kauzmann, W. *The Structure and Properties of Water*; Oxford University Press: New York, 1969.
(2) *Water: A Comprehensive Treatise*; Franks, F., Ed.; Plenum: New York, 1972−1979; Vols. 1−8.
(3) Sciortino, F.; Geiger, A.; Stanley, H. E. *Phys. Rev. Lett.* **1990**, *65*, 3452.
(4) Svishchev, I. M.; Kusalik, P. G. *J. Chem. Phys.* **1993**, *99*, 3049.
(5) Yeh, Y. L.; Mou, C. Y. *J. Phys. Chem. B* **1999**, *103*, 3699.
(6) Jedlovszky, P.; Mezei, M.; Vallauri, R. *Chem. Phys. Lett.* **2000**, *318*, 155.
(7) Hille, B. *Ionic Chanels of Excitable Membranes*; Sinauer Associates: Sunderland, 1992.
(8) Finkelstein, A. *J. Gen. Physiol.* **1976**, *68*, 127.
(9) *Physiology*; Berne, R. M., Levy, M. N., Koeppen, B. M., Stanton, B. A., Eds.; Mosby: St. Louis, 1998.
(10) Venable, R. M.; Zhang, Y.; Hardy, B. J.; Pastor, R. W. *Science* **1993**, *262*, 223.
(11) Heller, H.; Schaefer, M.; Schulten, K. *J. Phys. Chem.* **1993**, *97*, 8343.
(12) Marrink, S. J.; Berendsen, H. J. C. *J. Phys. Chem.* **1994**, *98*, 4155.
(13) Robinson, A. J.; Richards, W. G.; Thomas, P. J.; Hann, M. M. *Biophys. J.* **1995**, *68*, 164.
(14) Tu, K.; Tobias, D. J.; Klein, M. L. *Biophys. J.* **1995**, *69*, 2558.
(15) Tieleman, D. P.; Berendsen, H. J. C. *J. Chem. Phys.* **1996**, *105*, 4871.
(16) Gabdoulline, R. R.; Vanderkooi, G.; Zheng, C. *J. Phys. Chem.* **1996**, *100*, 15942.
(17) Hyvönen, M. T.; Rantala, T. T.; Ala-Korpela, M. *Biophys. J.* **1997**, *73*, 2907.
(18) Pasenkiewicz-Gierula, M.; Takaoka, Y.; Miyagawa, H.; Kitamura, K.; Kusumi, A. *J. Phys. Chem. A* **1997**, *101*, 3677.
(19) Husslein, T.; Newns, D. M.; Pattnaik, P. C.; Zhong, Q.; Moore, P. B.; Klein, M. L. *J. Chem. Phys.* **1998**, *109*, 2826.
(20) Pasenkiewicz-Gierula, M.; Takaoka, Y.; Miyagawa, H.; Kitamura, K.; Kusumi, A. *Biophys. J.* **1999**, *76*, 1228.
(21) Smondyrev, A. M.; Berkowitz, M. L. *J. Chem. Phys.* **1999**, *111*, 9864.
(22) Duong, T. H.; Mehler, E. M.; Weinstein, H. *J. Comput. Phys.* **1999**, *151*, 358.
(23) Bandyopadhyay, S.; Tarek, M.; Klein, M. L. *J. Phys. Chem. B* **1999**, *103*, 10075.
(24) Jedlovszky, P.; Mezei, M. *J. Chem. Phys.* **1999**, *111*, 10770.
(25) Jedlovszky, P.; Mezei, M. *J. Am. Chem. Soc.* **2000** *122*, 5125.
(26) López Cascales, J. J.; García de la Torre, J.; Marrink, S. J.; Berendsen, H. J. C. *J. Chem. Phys.* **1996**, *104*, 2713.
(27) Alper, H. E.; Bassolino, D.; Stouch, T. R. *J. Chem. Phys.* **1993** *98*, 9798.
(28) Alper, H. E.; Bassolino-Klimas, D.; Stouch, T. R. *J. Chem. Phys.* **1993** *99*, 5547.
(29) Feller, S. E.; Zhang, Y.; Pastor, R. W. *J. Chem. Phys.* **1995** *103*, 10267.
(30) Pastor, R. W. *Curr. Opin. Struct. Biol.* **1994** *4*, 486 and references therein.
(31) Mezei, M. MMC Program at URL: http://inka.mssm.edu/∼mezei/mmc.
(32) Schlenkirch, M.; Brickmann, J.; MacKerrel, A. D., Jr.; Karplus, M. In *Biological Membranes*; Merz, K. M., Roux, B., Eds.; Birkhäuser: Boston, 1996; pp 31−82.
(33) Jorgensen, W. L.; Chandrashekar, J.; Madura, J. D.; Impey, R.; Klein, M. L. *J. Chem. Phys.* **1983**, *79*, 926.
(34) Mezei, M. *J. Comput. Phys.* **1983**, *39*, 128.
(35) Jedlovszky, P.; Mezei, M. at URL: http://inka.mssm.edu/∼mezei/scri.
(36) Jedlovszky, P.; Mezei, M. *Mol. Phys.* **1999**, *96*, 293.
(37) Petrache, H. I.; Tristam-Nagle, T.; Nagle, J. F. *Chem. Phys. Lipids* **1998**, *95*, 83.
(38) Jedlovszky, P.; Mezei, M. Manuscript in preparation.
(39) Jedlovszky, P.; Brodholt, J. P.; Bruni, F.; Ricci, M. A.; Soper, A. K.; Vallauri, R. *J. Chem. Phys.* **1998**, *108*, 8528.
(40) Jedlovszky, P. *J. Chem. Phys.* **1999**, *111*, 5975.
(41) Blum, L.; Torruela, A. J. *J. Chem. Phys.* **1972**, *56*, 303.
(42) Gray, C. G.; Gubbins, K. E. *Theory of Molecular Fluids*; Fundamentals, Vol. 1; Clarendon: Oxford, 1984.